Dynamic Contact Angles and Hydrodynamics near a Moving Contact Line

John A. Marsh[(a)] and S. Garoff
Department of Physics, Carnegie Mellon University, Pittsburgh, Pennsylvania 15213

E. B. Dussan V.
Schlumberger Doll Research, Old Quarry Road, Ridgefield, Connecticut 06877
(Received 28 December 1992)

The contact angle is an important boundary condition needed to predict the shape of menisci. However, its measurement and use under dynamic conditions are not well understood. We have measured the shape of menisci very close to moving contact lines over a suite of geometric shapes for the macroscopic menisci. The excellent agreement between theory and experiment establishes that the proposed boundary condition characterizes only the materials of the system. Implications for the microscopic physics controlling the dynamic contact angle are explored.

PACS numbers: 68.10.Gw, 68.10.Cr, 68.45.Gd

The most commonly used macroscopic characterization quantifying the wettability of a material system (two immiscible fluids and a solid surface) is the *contact angle*. This is because the contact angle boundary condition frequently plays a critical role in determining the meniscus shape. It is the shape of the meniscus that actually quantifies the degree to which a particular liquid wets a solid surface. The difficulty with this characterization arises in the measurement of the contact angle under *dynamic* conditions. This is a direct consequence of the large curvature of the meniscus (compared to the static case) very close to even a slowly moving contact line, resulting from dynamic forces [1–6]. We present experimental data which carefully quantify the dynamic contact angle boundary condition for a particular material system. This represents the first time in which this boundary condition has been measured for the same material system over a suite of geometries of the macroscopic meniscus.

The situation is further complicated by the lack of understanding of the physics governing the behavior of the fluids in the immediate vicinity of the moving contact line. This is true from both a molecular and continuum perspective. As a consequence, no general consensus exists of how to quantify the influence of the hydrodynamic forces on the meniscus shape in the microscopic region near the moving contact line (on the submicron scale) [4,7]. Even without this knowledge, the existence of a well-defined dynamic contact angle boundary condition has been argued [3,8,9]. It is restricted to situations in which the overall size of the meniscus is much larger than a micron, and the capillary number is relatively small. Briefly, the boundary condition consists of specifying the *asymptotic* form of the slope of the interface, θ, as $r \to 0$, where r is the distance to the contact line. (In contrast, for the static case, the value of θ is specified only at the contact line, $r=0$.) The asymptotic form is

$$\theta(r) = g^{-1}(\mathrm{Ca} \ln r/L) . \quad (1)$$

Here, Ca denotes the capillary number $U\mu/\sigma$, where U is the speed of the contact line, μ is the viscosity of the liquid, and σ is the surface tension; L is the parameter [equivalent to $R \exp[-g(\theta_R)/\mathrm{Ca}]$ in [9], implying equivalence to $L_S \exp[-g(\theta_{\mathrm{act}})/\mathrm{Ca}]$, where θ_R is the value of θ at $r=R$ and θ_{act} is the "actual" or "microscopic" contact angle and L_S is the slip length] having the dimension of length, which can be determined from experiments; and $g(x) \equiv \int_0^x \{(y - \cos y \sin y)/2 \sin y\} dy$. (This includes the simplification that the second fluid in this study is a gas whose dynamics can be ignored.)

Thus, the objective of this study consists of determining the validity of using (1) as a boundary condition for the meniscus shape under dynamic conditions. We compare experimental measurements of $\theta(r)$ over a range of values of r close to the moving contact line to predictions obtained from a mathematical solution of the shape of the meniscus which uses (1) as a boundary condition. An important aspect of our study is that this comparison is made using the *same* material system in more than one geometry. This last step is essential when evaluating whether (1) is a characterization of only the *materials* of the system. Disagreement in $\theta(r)$ between theory and experiment would have far-reaching implications. For instance, it would bring into question the validity of almost all the physical models of the dynamic behavior of the fluids in the immediate vicinity of the moving contact line developed over the past fifteen years [9].

A suite of experiments was performed using an arrangement similar to that of [9]. We immersed a 2.54 cm outer diameter Pyrex cylindrical tube, at a constant speed, into a beaker of polydimethylsiloxane (PDMS) polymer melt (see Fig. 1). This geometry possesses the largest length scale, the capillary length, associated with the macroscopic meniscus. The tube was tilted at an angle α relative to the horizontal, and translated along its axis. The slope of the interface $\theta(r)$ was measured close to the moving contact line situated on the surface of the tube. The air-oil interface was just above the lip of the beaker, making $\theta(r)$ directly measurable. The experiments were performed over a range of immersion speeds

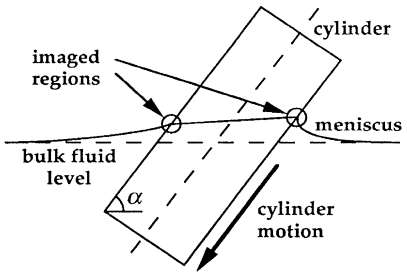

FIG. 1. Schematic of the apparatus showing the immersed cylinder geometry for viewing the meniscus shape near the moving contact line. The immersion angle is α as shown for the imaged region on the left, and $180° - \alpha$ for that on the right.

($1.5\ \mu$m/s to $350\ \mu$m/s, giving Ca from 7×10^{-5} to 2×10^{-2}) in order to assess the influence of the contact line speed on the dynamic contact angle boundary condition. They were then repeated over a range of α ($60° < \alpha < 120°$) to determine the influence of geometry on the boundary condition, each α resulting in a different geometry of the silicon oil (not done in [9]).

The Pyrex tube was fire polished and carefully cleaned so that the contact line moved smoothly across its surface. The PDMS had a viscosity $\eta = 1030$ cP, surface tension $\sigma = 20.8$ dyn/cm, and density $\rho = 0.970$ g/cm^3. Using ellipsometry, we found no thin film in front of the bulk meniscus after a time comparable to that of our experiments.

Images of the meniscus profile were obtained using a long working distance microscope and a high resolution charge-coupled device camera, and were digitized on a microcomputer. Koehler illumination conditions ensure an even background illumination and optimal resolution. Alignment of the microscope, cylinder axis, and gravity were crucial and were better than 0.5°. The digitized images had a resolution of about 1 μm per pixel. A sample image is shown in Fig. 2. Photos of static menisci, where the interface shape is well known, were used to calibrate the smallest distance from the contact line where the image of the interface shape was undistorted. The inner cutoff distance is sensitive to the details of the back lighting, and an optimal set of lighting parameters was established so that all the data for $r > 20\ \mu$m from the contact line were usable.

Transformation of the data into polar coordinates suitable for comparison with theory involved finding the contact line position and correcting for misalignment of the pixel columns with true vertical and for geometric distortions. By combining data from five images, we formed data sets containing 3000 points. Our techniques generated a more accurate and complete set of data than interference techniques [10].

We compared the experimental measurements of the slope to the local form of the mathematical solution derived using (1) as a boundary condition [9],

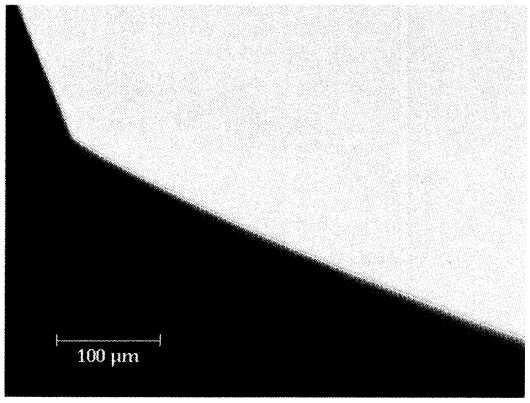

FIG. 2. A typical image. The white row of pixels represents the location of the edge of the tube and the interface as determined by image analysis.

$$\theta(r) = g^{-1}\left(\mathrm{Ca}\ln\frac{r}{L}\right) + f(r/a) - \omega_0\,, \tag{2}$$

where

$$\omega_0 \equiv g^{-1}(\mathrm{Ca}\ln a/L)\,. \tag{3}$$

Here, a denotes the capillary length, $\sqrt{\sigma/\rho\tilde{g}}$, where $\tilde{g}$ is the gravitational constant and $f(r/a)$ represents the contribution dependent upon the geometry of the system, depending explicitly upon the parameters ω_0, a/R_T, and α, R_T denoting the outer radius of the Pyrex tube [9]. The only unknown in (2), L, was determined using least-squares minimization.

Shown in Fig. 3 are typical fits for two different values of α. The overall agreement with the theory is excellent. When the errors on the individual data points are taken to be uniformly $\pm 1.0°$ the reduced χ^2 values are typically about 1. Data are also presented in the region $10\ \mu\mathrm{m} < r < 20\ \mu$m, which systematically deviates from the fit; however, we have reason to believe, as stated above, that these data contain distortions introduced by optical effects. Note that the slope changes most rapidly as the contact line is approached. This is the effect of the relatively large size of the viscous forces acting on the interface shape in this region, represented by the first term on the right-hand side of (2). This term constitutes 95% and 97% of $\theta(r)$ within the region $r < 50\ \mu$m, for $\alpha = 70°$ and 120°, respectively. Thus, our measurements lie just a little outside the region where the interface is free from the geometry dependence represented by the last two terms in (2).

A further consequence of this comparison is the experimental determination of L as a function of contact line speed U. The values of L determined over our entire suite of experiments are summarized in Fig. 4. To within experimental error, L is independent of α. The relatively large uncertainty in L at a given value of U results in an

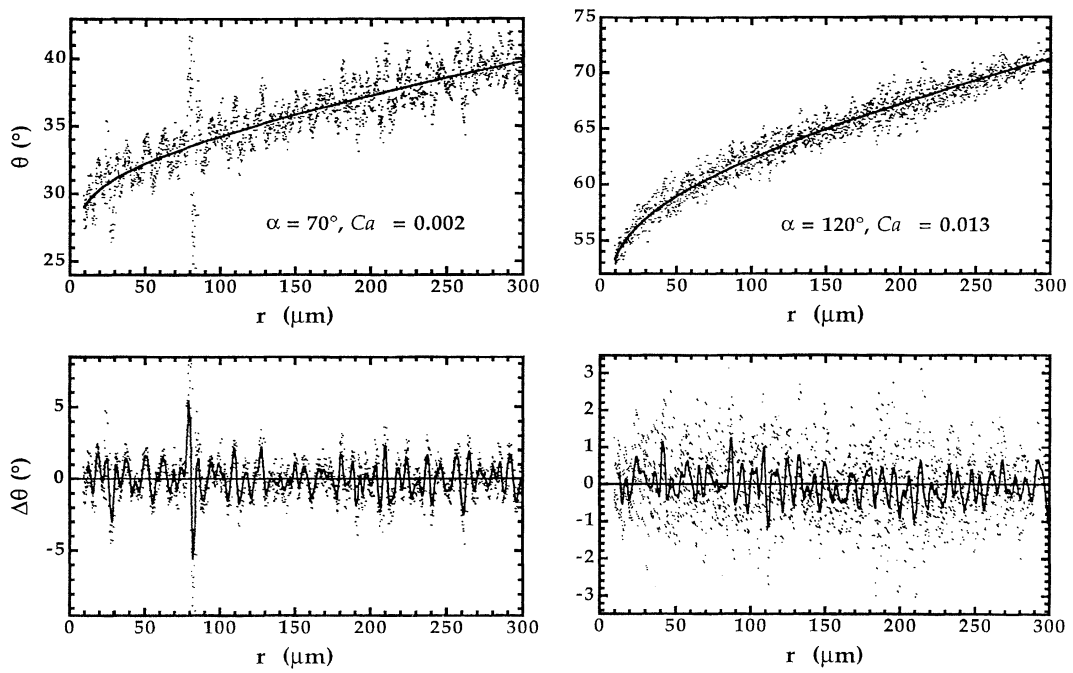

FIG. 3. The dependence of the slope of the interface θ on the distance from the moving contact line r for two different values of α. The solid line is the fitted theoretical curve. Also plotted below each case is the difference between the measured value of θ and theory, $\Delta\theta$. The solid curve represents a running average over 5 μm. In both cases, no systematic deviation is evident except in the region 10 μm $< r <$ 20 μm and the "spike" at about $r = 80$ μm for $\alpha = 70°$ which is due to dust in the microscope.

uncertainty of less than $\pm 1°$ in $\theta(r)$, a direct consequence of L appearing only within the logarithm and the function g. Thus, our measurements represent a significant data set establishing the validity of (1) for this particular material system.

Our approach to quantifying the wettability of a material system under dynamic conditions can be contrasted to the usual procedure found in the literature. Usually the "apparent contact angle" is determined over a range of contact line speeds [4]. The apparent contact angle is the contact angle formed by the *static* meniscus shape which best approximates the shape of the meniscus *far* from the contact line under dynamic conditions. The word "apparent" refers to the fact that it it not an "actual" slope at a particular position on the meniscus. For our experimental geometry, it can be shown that the apparent contact angle is ω_0. It is of fundamental importance to note that (1) implies the apparent contact angle is *not* a material property. This is a consequence of the appearance of the capillary length a in (3). Hence, the usual approach of characterizing dynamic wettability does not use a geometry-free parameter. Furthermore, Eq. (3) can be used to extract the material property $L(U)$, for a particular material system, *only* after the validity of (1) has been established by measuring $\theta(r)$ as $r \rightarrow 0$. A materials characterization cannot be achieved by restricting measurements of the shape of the meniscus to the region far from the moving contact line. This problem can be further elucidated by considering the case of flow through a capillary tube, by far the most common geometry used for measuring the apparent contact angle. In this case, the apparent contact angle $\tilde{\omega}_0$ is the contact angle formed by a spherical-cap-shaped meniscus. For material systems in which the validity of (1) has been established, $L(U)$ can be determined using the expression $\tilde{\omega}_0 \equiv g^{-1}(\mathrm{Ca} \ln \tilde{R}_T/L)$, where $\tilde{R}_T$ denotes the *inner* diameter of the capillary. Here, the dependence of the apparent contact angle on the geometry is evident by the presence of $\tilde{R}_T$.

Our results have implications concerning the physics governing the dynamics of the fluids in the immediate vi-

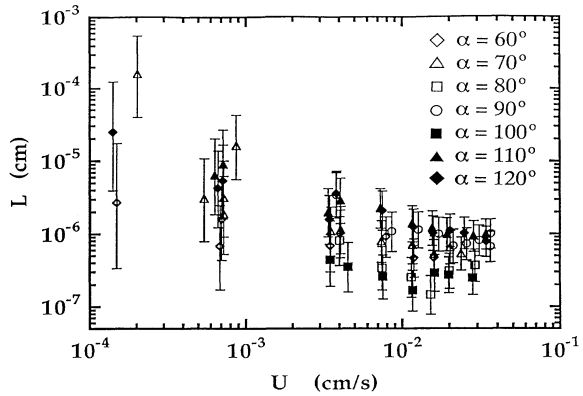

FIG. 4. The value of the parameter L for the suite of experiments.

cinity of the moving contact line on the microscopic length scale. The strongest conclusion is that whatever the physics, it must produce an interface shape with slope obeying (1) away from the immediate vicinity of the contact line. As discussed in detail elsewhere [9], various mechanisms are consistent with (1), including a plethora of models resulting in viscous fluids slipping at the surface of the solid very close to the moving contact line as well as models assuming the presence of a thin film of liquid on the solid surface [7,11]. For example, two parameters are introduced in the case of the slip models: a slip length L_S and the "actual" contact angle θ_{act} (both may depend on U), related to L by $\theta_{act}=g^{-1}(\mathrm{Ca}\times\ln L_S/L)$. This relationship represents the extent to which L_S and θ_{act} can be determined using our "macroscopic" measurements. However, from this we can conclude that either θ_{act} and/or L_S must depend upon U, for if they were both independent of U, implying $\theta_{act}=0$ for our material system, then the above relationship implies L is *independent* of U, which is inconsistent with Fig. 4. By further demanding that θ_{act} maintain its static advancing value under dynamic conditions, a common assumption supported by recent molecular dynamics simulations [12], again implying $\theta_{act}=0$ for our material system, then $L_S=L$. Figure 4 can then be used to determine the values of L_S at various values of U. Here, the relatively large experimental uncertainty in L results in a large error in the prediction of L_S. Finally, it is of interest to note that the apparent contact angle, to the accuracy of our experiments, follows a power law in Ca of the form $\omega_0=(296^\circ\pm4^\circ)\mathrm{Ca}^{0.347\pm0.002}$ over our entire range of Ca. However, we note that (3) and any U-dependent L imply that the apparent contact angle *cannot* follow a power law in Ca. The power law we observe is a consequence of a combination of the finite accuracy of our experiments and the weak dependence of L on U in Fig. 4.

In summary, a significant set of data has been presented which substantiates the validity of (1) when moving contact lines are present for the material system consisting of silicone oil-air-Pyrex and at capillary numbers less than 10^{-2}. This represents both a boundary condition for determining the dynamic behavior of a macroscopic fluid body and a constraint on acceptable models of the behavior of the fluids in the immediate vicinity of the moving contact line. Measurements were made of the slope of the interface over a range of r close to the moving contact line, where viscous forces are important, the measurement of only the dynamic behavior of the apparent contact angle being insufficient. The material parameter appearing in (1), L, was determined for U over the range $1.5\ \mu\mathrm{m/s}<U<350\ \mu\mathrm{m/s}$. The behavior of L in conjunction with (1) may be regarded as a fundamental characterization of the wettability of a material system under dynamic conditions. We do not anticipate a change in the validity of (1) for material systems having a nonzero advancing contact angle. However, this is the subject of ongoing research.

We wish to thank M. Chaudhury of Dow Corning for providing coatings for some of our samples and M. O. Robbins for valuable discussions. This work was supported by a Link Foundation Fellowship, the Petroleum Research Fund, and the National Science Foundation Grant No. DMR 91-13152.

[a]Present address: Physique de la Matière Condensée, College de France, 75231 Paris CEDEX 05, France.

[1] V. O. Voinov, Fluid Dyn. **11**, 714 (1976).
[2] R. J. Hansen and T. Y. Toong, J. Colloid Interface Sci. **37**, 196 (1971).
[3] F. Y. Kafka and E. B. Dussan V., J. Fluid. Mech. **95**, 539 (1979).
[4] E. B. Dussan V., Annu. Rev. Fluid Mech. **11**, 371 (1979).
[5] J. Lowndes, J. Fluid. Mech. **101**, 631 (1980).
[6] C. G. Ngan and E. B. Dussan V., J. Fluid. Mech. **118**, 27 (1982).
[7] P. G. de Gennes, Rev. Mod. Phys. **57**, 827 (1985).
[8] C. G. Ngan and E. B. Dussan V., J. Fluid. Mech. **209**, 191 (1989).
[9] E. B. Dussan V., E. Ramé, and S. Garoff, J. Fluid. Mech. **230**, 97 (1991).
[10] J. D. Chen and N. Wada, J. Colloid Interface Sci. **148**, 207 (1992).
[11] P. G. de Gennes, X. Hua, and P. Levinson, J. Fluid. Mech. **212**, 55 (1990).
[12] P. A. Thompson and M. O. Robbins, Phys. World **3**, 35 (1990).

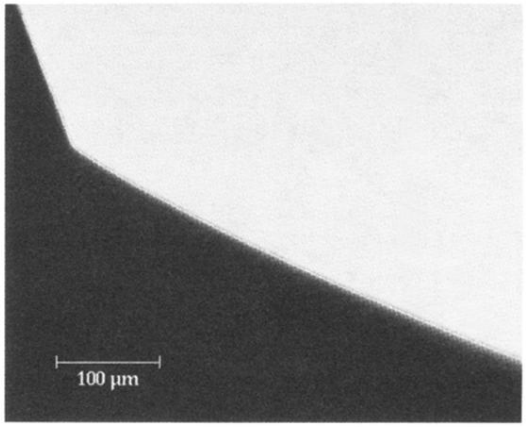

FIG. 2. A typical image. The white row of pixels represents the location of the edge of the tube and the interface as determined by image analysis.